# Polymer Chemistry

Accepted Manuscript






ROYAL SOCIETY OF CHEMISTRY

www.rsc.org/polymers

Journal Name

RSCPublishing

ARTICLE

# $CO_2$- and thermo-responsive vesicles: from expansion-contraction transformation to vesicles-micelles transition

Cite this: DOI: 10.1039/x0xx00000x

Received 00th January 2012,
Accepted 00th January 2012

DOI: 10.1039/x0xx00000x

www.rsc.org/

Hui Zou[a] and Weizhong Yuan*[a,b]

The amidine- and dimethylaminoethyl-containing block copolymer PADS-*b*-PDMAEMA was prepared by the combination of reversible addition-fragmentation chain transfer polymerization and click chemistry. Benefitting from the amphiphilic nature, the PADS-*b*-PDMAEMA copolymer could spontaneously form vesicles in water when the concentration is above the critical aggregation concentration. As the amidine and dimethylamino units in the copolymer are both typical $CO_2$ responsive chemical groups, the PADS-*b*-PDMAEMA copolymer vesicles presented unique dual $CO_2$ responses. Meanwhile, the vesicles also showed thermo-responsive behaviours due to the thermal response of PDMAEMA block. And the lower critical solution temperature (LCST) of the copolymer in aqueous solution is 42.8°C. The size and morphologies of these vesicles can be adjusted by controlling the protonation/deprotonation of amidine and dimethylamino species through bubbling $CO_2$ or Ar. Alternating treatment with $CO_2$ and Ar could realize a reversible expansion-contraction transformation of these vesicles. Moreover, the reversible vesicles-micelles transition could also be achieved through stimuli of temperature and gas. Due to the $CO_2$- and thermo-responsive properties, the PADS-*b*-PDMAEMA visicles were used as a carrier for drug delivery systems. Doxorubicin (DOX), an anticancer drug, was used as a model drug and loaded into the vesicles. The vesicles presented good controlled release behaviour. The release rate and level could be controlled through bubbling $CO_2$ and changing temperature.

## Introduction

Considerable attention has been paid to the stimuli-responsive polymeric self-assemblies due to their potential applications in biomedical and nanotechnology fields, such as drug delivery systems to achieve the controlled release and reduce the side effects of drugs.[1-4] Especially, those polymeric self-assemblies containing dual responses originated from hydrophilic and hydrophobic parts respectively are attracting the interest because they could achieve more obvious change of morphologies than those containing single response from hydrophilic part, such as reversible assembly-disassembly and micelle-vesicle transitions.[5-7] It is clear that these self-assembly systems would be beneficial to the multiply controlled release of loaded drug.[8-10]

Nowadays, carbon dioxide ($CO_2$) has attracted great attention owing to its availability, nontoxicity, biocompatibility, low cost and abundance. Various reversible $CO_2$-responsive materials have been investigated and reported, including organogels,[11] supramolecular polymers,[12] polymeric vesicles[13] and organic-inorganic hybrid nanomaterils,[14] which utilized a reversible reaction between $CO_2$ and amines. Feng *et al.* prepared an amidine-based $CO_2$-responsive polymer with amidine pendants derived from polystyrene and investigated the hydrophobic-hydrophilic transition behaviour of the polymer upon the stimulus of $CO_2$.[15] Gnanou *et al.* reported that $CO_2$ could reversibly react with poly(N-heterocyclic-carbene)s to form relatively air-stable poly(NHC-$CO_2$) adducts and studied its use in organocatalysis.[16] Yuan *et al.* prepared a series of amphiphilic block copolymer composed of poly(ethylene glycol) (PEG) and poly(N-amidino)dodecyl acrylamide (PAD) and found that its self-assembled polymersome could reversibly respond to $CO_2$, presenting a distinctive breathing function.[17] Most of the $CO_2$-responsive materials containing amidine functional group could react with $CO_2$ and water to form charged amidinum bicarbonates.[18-21] The hydrophobic amidine groups would be transferred into hydrophilic amidinum bicarbonate after filling $CO_2$. Moreover, as a pH and temperature dual responsive polymer, poly(N,N-dimethylaminoethyl methacrylate) (PDMAEMA) could react directly with $CO_2$ in water without functionalization with

amidine.[22-25] And the value of lower critical solution temperature (LCST) of PDMAEMA increased drastically after bubbling $CO_2$.

Herein, in this paper, the block copolymer containing amidine groups (PADS) and PDMAEMA was synthesized by the combination of reversible addition-fragmentation chain transfer polymerization (RAFT) and click reaction (Scheme 1). As an amphiphilic copolymer, PADS-*b*-PDMAEMA could spontaneously form vesicles in water. Since the amidine and dimethylamino functionalities in the PADS-*b*-PDMAEMA copolymer are both $CO_2$ responsive chemical groups, the PADS-*b*-PDMAEMA self-assembled vesicles presented unique dual $CO_2$ responses. At the same time, the vesicles also showed thermo-responsive properties resulting from the thermal response of PDMAEMA block. Thus the vesicles presented excellent $CO_2$- and thermo-responsive properties (Scheme 2). To assess the suitability of the PADS-*b*-PDMAEMA vesicles as a carrier for controlled drug release, drug release studies were performed using DOX as the model drug. The results showed that the release rate and level can be controlled through bubbling $CO_2$ and changing temperature. These properties make such $CO_2$- and thermo-responsive vesicles potential candidates to be used in novel intelligent delivery systems and smart biomaterial fields.

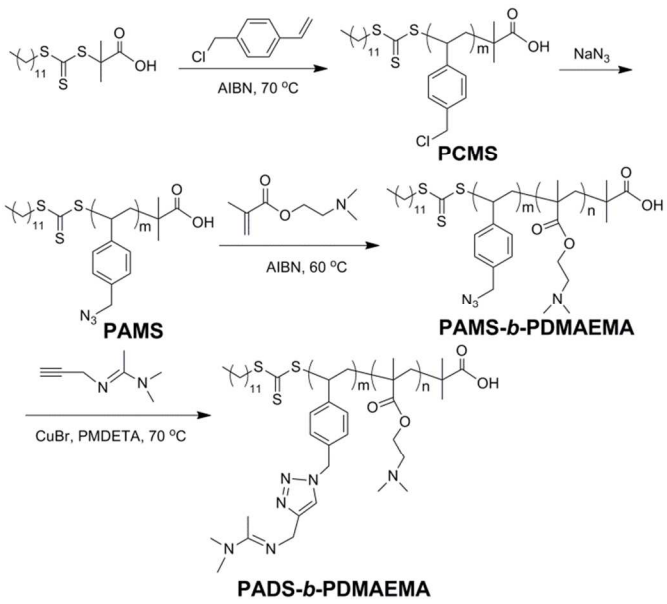


**Scheme 1** Synthesis of the PADS-*b*-PDMAEMA copolymer.

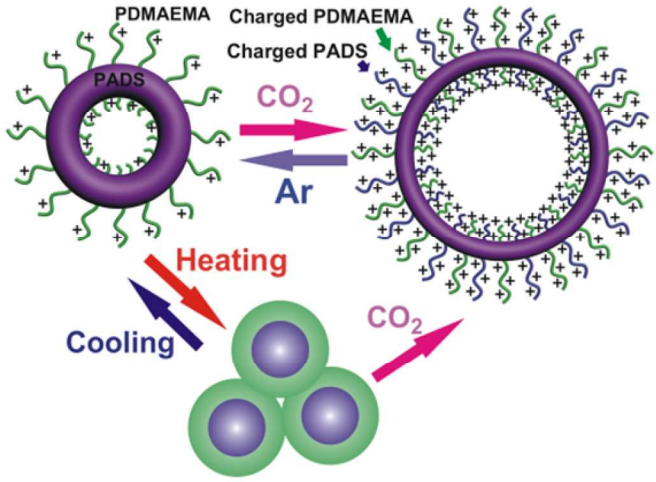


**Scheme 2** Self-assembly of PADS-*b*-PDMAEMA into vesicles and the reversible vesicles-micelles/aggregates transformation under bubbling $CO_2$/Ar and heating/cooling conditions (top) and gas-switchable structural change of PADS and PDMAEMA segments (bottom).

## Experimental

### Materials

S-dodecyl-S'-(α,α'-dimethyl-α''-acetic acid) trithiocarbonate (DDMAT) was synthesized according to the literature.[26] 2,2'-Azobisisobutyronitrile (AIBN, Aldrich, 98%) was recrystallized from ethanol. N'-Propargyl-N,N-dimethylacetamidines (PDAA) was prepared according to the literature.[18] p-Chloromethylstyrene (CMS) (Aldrich, 90%) was purified by vacuum distillation from $CaH_2$. N,N,N',N'',N''-Pentamethyl diethylenetriamine (PMDETA) (Acros Oganic, 99%), N,N-dimethylacetamide dimethyl acetal (Alfa Aesar), propargyl amine (Alfa Aesar) and sodium azide ($NaN_3$, Alfa Aesar) were used as received. Copper bromide (CuBr, Alfa Aesar, 99%) was treated by stirring in glacial acetic acid and washed with ethanol several times. 2-(N,N-dimethylamino) ethyl methacrylate (DMAEMA, Acros Organic, 99%) was dried over CaH2 and distilled under reduced pressure. All other reagents were purchased from Shanghai Chemical Reagent Co. Ltd., and used as received unless otherwise specified.

### Characterization

**Nuclear Magnetic Resonance (NMR).** $^1$H NMR spectra of samples were obtained from a Bruker AVANCE-400MHz NMR spectrometer with $CDCl_3$ and DMSO-$d_6$ as solvents. The chemical shifts were relative to tetramethylsilane.

**Attenuated total internal reflectance fourier transform infrared (ATR FTIR).** ATR FTIR spectra of samples were recorded on an EQUINOSS/HYPERION2000 spectrometer (Bruker, Germany).

**Gel Permeation Chromatography (GPC).** GPC analysis was carried out with a HLC-8320 (Tosoh, Japan) analysis system with two columns (TSK gel super AWM-H×2, R0091+R0093), using DMF with 10 mM LiBr as eluents at a

flow rate of 0.6 mL $min^{-1}$ at 40°C. PS calibration kit was used as the calibration standard.

**Dynamic Light Scattering (DLS).** Morphology of the micelles/aggregates of brush polymers in water was investigated using DLS techniques. The experiments were performed on a Malvern Autosizer 4700 DLS spectrometer. DLS was performed at a scattering angle 90°. The $R_h$ was obtained by a cumulant analysis.

**Transmission Electron Microscopy (TEM).** The morphology of brush polymers micelles/aggregates was observed with a JEOL JEM-2010 TEM at an accelerating voltage of 120 kV. The samples for TEM observation were prepared by placing 10 μL of the vesicular or micellar solutions on copper grids coated with thin films and carbon.

**ζ-Potentiometer (ζ-PM).** A ζ-potentiometer (Zeta-potentiometer, Zetasizer Nano ZS90 instrument, Malvern Instruments) was used to measure the ζ-potential of the fully dialyzed vesicular solutions. The potential was determined in aqueous solution at 25°C with a given gas stimulus.

**Optical transmittances.** The optical transmittances of the copolymer aqueous solutions at various temperatures were measured at a wavelength of 500 nm using a UV-visible spectrophotometer (U-3310, Hitachi). The temperature of the sample cell was thermostatically controlled using an external superconstant temperature bath. The solutions were equilibrated for 10 min at each measuring temperature. The LCST values of the copolymer aqueous solutions were defined as the temperature producing a 50% decrease in optical transmittance.

**Fluorescence Spectroscopy (FS).** The critical aggregation concentration (CAC) of the copolymer PADS-*b*-PDMAEMA was measured by an F-2500 (Hitachi, Japan) fluorescence spectrophotometer with a xenon lamp source.

### Synthesis of poly(*p*-chloromethylstyrene) (PCMS)

PCMS was synthesized by RAFT with DDMAT as the RAFT agent. DDMAT (0.362 g, 1.0 mmol), *p*-chloromethylstyrene (3.05 g, 20.0 mmol) and AIBN (32.8 mg, 0.2 mmol) were dissolved in anisole (2 mL). The mixture was degassed with three freeze-evacuate-thaw cycles. The polymerization reaction was performed at 70°C for 24 h. Then, the product mixture was diluted by the same volume of dry THF, and the final product was obtained by precipitation in *n*-hexane and drying under vacuum for 24 h (Yield: 81%). $M_{n,NMR}$=1887 g/mol, $M_{n,GPC}$=2010 g/mol, $M_w/M_n$=1.22. ATR FTIR ($cm^{-1}$): 2840-3020 ($\nu_{C-H}$). $^1$H NMR (DMSO-$d_6$, $\delta$, ppm): 6.28-7.38 (arom. C*H* of styrenic ring), 4.68 (C$H_2$Cl), 0.78-1.88 ($C_{11}H_{23}$, C$H_2$C*H*, C(C$H_3$)$_2$).

### Synthesis of poly(*p*-azidomethylstyrene) (PAMS)

PCMS (1.51 g, 0.8 mmol) was dissolved in dry DMF (30 mL) and then $NaN_3$ (2.60 g, 40 mmol) was added. The reaction mixture was stirred at room temperature for 48 h and then precipitated in excess of water. The obtained crude product was re-dissolved in dichloromethane and re-precipitated in cold methanol. The resultant white solid was collected by filtration and dried in a vacuum oven for 48 h (Yield: 88%). $M_{n,NMR}$= 1964 g/mol. ATR FTIR ($cm^{-1}$): 2840-3020 ($\nu_{C-H}$), 2100 ($\nu_{azide\ group}$). $^1$H NMR (DMSO-$d_6$, $\delta$, ppm): 6.34-7.29 (arom. C*H* of styrenic ring), 4.35 (C$H_2$N$_3$), 0.71-1.91 ($C_{11}H_{23}$, C$H_2$C*H*, C(C$H_3$)$_2$).

### Synthesis of PAMS-*b*-PDMAEMA copolymer

The copolymer of PAMS-*b*-PDMAEMA was synthesized by RAFT with PAMS as the macro RAFT agent. PAMS (0.189 g, 0.1 mmol), DMAEMA (1.5 g, 9.5 mmol) and AIBN (3.0 mg, 0.02 mmol) were dissolved in dry DMF (4 mL). The mixture was degassed with three freeze-evacuate-thaw cycles. The polymerization reaction was performed at 60°C for 24 h. Then, the product mixture was diluted by dry THF, and the final product was obtained by precipitation in cold *n*-hexane three times and drying under vacuum for 48 h (Yield: 72%). $M_{n,NMR}$=4786 g/mol, $M_{n,GPC}$=4990 g/mol, $M_w/M_n$=1.26. $^1$H NMR (DMSO-$d_6$, $\delta$, ppm): 4.35 (C$H_2$N$_3$), 3.99 (OC$H_2$CH$_2$N), 2.50 (OCH$_2$C$H_2$N), 2.19 (N(C$H_3$)$_2$), 1.16-1.93 ($C_{11}H_{23}$, C$H_2$C*H*, C(C$H_3$)$_2$, C(CH$_3$)C*H*), 0.69-0.99 (C(C$H_3$)CH).

### Synthesis of PADS-*b*-PDMAEMA copolymer

The copolymer of PADS-*b*-PDMAEMA was synthesized by click reaction of alkynyl groups of PAMS with PAMS (Scheme S1). PAMS-*b*-PDMAEMA (0.6 g, 0.1231 mmol) and PDAA (0.305 g, 2.462 mmol) were dissolved in dry DMF (10 mL). Then, CuBr (0.354 g, 2.462 mmol) and PMDETA (0.492 g, 2.462 mmol) were added. The mixture was degassed with three freeze-evacuate-thaw cycles. The click reaction was performed at 50°C for 12 h. After being cooled to room temperature, the reaction flask was opened to air, and the crude product was diluted with THF and passed through a neutral oxide alumina column to remove the copper catalysts. The polymer was obtained by precipitation in *n*-hexane and dried *in vacuo* for 48 h (Yield: 61%). $M_{n,NMR}$=6040 g/mol. $^1$H NMR (DMSO-$d_6$, $\delta$, ppm): 5.30 (C$H_2$-N-N), 3.99 (OC$H_2$CH$_2$N, C$H_2$-N=C), 3.11 (C-N(C$H_3$)$_2$), 2.50 (OCH$_2$C$H_2$N), 2.19 (N(C$H_3$)$_2$), 1.35-1.93 ($C_{11}H_{23}$, C$H_2$C*H*, C(C$H_3$)$_2$, C(CH$_3$)C*H*, N=C(C$H_3$)), 0.66-1.04 (C(C$H_3$)CH).

### Self-assembly of PADS-*b*-PDMAEMA

30 mg of PADS-*b*-PDMAEMA was dissolved in THF (4 mL). Then deionized water was added at a rate of 1 mL $h^{-1}$ under vigorous stirring until the solution was changed from transparent to translucent. Then the solution was dialyzed against water with a dialysis tube (molecular weight cut-off: 3500 Da) at 25°C for 72 h.

### Preparation of DOX-loaded PADS-*b*-PDMAEMA vesicles

In this experiment, the anti-cancer drug of DOX was chosen to be used as the model drug. The mixture of DOX•HCl (15 mg), $Et_3N$ (3 mL) and dry DMF (10 mL) was stirred at room temperature overnight. Then 50 mg of PADS-*b*-PDMAEMA copolymer was added. After stirring for 6 hours, the mixture was dialyzed against water with a dialysis tube (molecular weight cut-off: 3500 Da) at 25 °C for 24 h and replaced with fresh water at the interval of 6 h.

**DLE and DLC measurements of the vesicles**

Measurement of the standard curve of DOX: preparing a series of DOX aqueous solutions with different concentrations and measuring the UV absorption intensity at the wavelength of 497 nm. To take 1 mL of vesicle solution loading DOX (1.0 mg/mL) and freeze-dried the solution, the dried vesicle were obtained. Then, 2 mL of DMF was added to dissolve the vesicles, and the vesicles were destroyed which led to the complete release of DOX. Then, the drug loading efficiency (DLE) and drug loading content (DLC) could be calculated according to the following formulae:

DLC (wt%)=(weight of loading DOX/weight of copolymer) × 100%

DLE (wt%)=(weight of loading DOX/weight of DOX in feed) × 100%

***In vitro* release of DOX loaded in vesicles**

To take 2 mL of vesicle solution loading DOX (1.0 mg/mL) into the dialysis membrane (molecular weight cut-off: 3500 Da) and immerse it into 25 mL of PBS (pH 7.4, 10 mM). At the set interval, 2 mL of release solution was withdrawn and replaced by 2 mL of fresh PBS. The cumulative release amount (E) was calculated according to the following formulae:

$$\mathrm{E} = \frac{V_e \sum_1^{n-1} C_\mathrm{i} + V_0 C_\mathrm{n}}{\mathrm{m_{DOX}}}$$

Here, E was the cumulative release amount. $V_e$ was the replaced PBS volume (2 mL). $V_0$ was 25 mL. $C_n$ was the concentration of DOX after $n$ times replacements of PBS. And $m_{Dox}$ was the content of DOX loading in micelles.

## Results and discussion

**Synthesis of PADS-*b*-PDMAEMA**

The diblock copolymer PADS-*b*-PDMAEMA was synthesized by the combination of reversible addition-fragmentation chain transfer polymerization (RAFT) and click reaction as illustrated in Scheme 1. Comparing to the direct polymerization of polyamidine, the method based on click reaction is facile and efficient.

The PCMS was prepared by RAFT of CMS monomer using S-dodecyl-S'-(α,α'-dimethyl-α''-acetic acid) trithiocarbonate (DDMAT) as RAFT agent, and PAMS was obtained through reacting PCMS with excess $NaN_3$.The $^1$H NMR spectrum of PCMS is shown in Fig.1(a). All the proton signals of the polymer can be detected. Fig. 1(b) shows the $^1$H NMR spectrum of PAMS. It can be observed that the chemical shifts of the benzylic protons shifted from 4.68 ppm in PCMS (Fig. 1(a)) to 4.35 ppm in PAMS (Fig. 1(b)), indicating that all chloride groups have been substituted by azide groups. Furthermore, a comparison of the FT-IR spectra of PCMS and PAMS in Fig. 2 revealed the appearance of an absorbance peak at 2100 cm$^{-1}$ for PAMS, which is characteristic absorption peak of the azide group.[27-30]

PAMS-*b*-PDMAEMA was synthesized by RAFT of DMAEMA monomer with PAMS as the macro-RAFT agent. The $^1$H NMR spectrum of PAMS-*b*-PDMAEMA is shown in Fig. 3(a). Comparing the $^1$H NMR spectrum of PAMS-*b*-PDMAEMA (Fig. 3(a)) with that of PAMS (Fig. 1(b)), new peaks at 3.99 ppm (peak b in Fig. 3(a)), 2.19 ppm (peak d in Fig. 3(a)) and 0.69 ppm ~ 0.99 ppm (peak c in Fig. 3(a)) appeared in the spectrum of PAMS-*b*-PDMAEMA. These peaks are attributed to the PDMAEMA block.

Finally, the block copolymer containing amidine and dimethylaminoethyl groups (PADS-*b*-PDMAEMA) was prepared by click reaction between PDAA and PAMS-*b*-PDMAEMA. The $^1$H NMR spectrum of PDMS-*b*-PDMAEMA is shown in Fig. 3(b). We can observed that the chemical shifts of the benzylic protons (peak a in Fig. 3) shifted from 4.35 ppm in PAMS-*b*-PDMAEMA (Fig. 3(a)) to 5.30 ppm in PADS-*b*-PDMAEMA (Fig. 3(b)), suggesting that the "click" reaction was accomplished.

The GPC traces of PCMS and PDMS-*b*-PDMAEMA are shown in Fig. 4. It can be seen that the traces are mono-modal, suggesting that the pure polymers were obtained. The number-average molecular weights of PCMS and PDMS-*b*-PDMAEMA were 2010 g mol$^{-1}$ and 4990 g mol$^{-1}$, respectively.

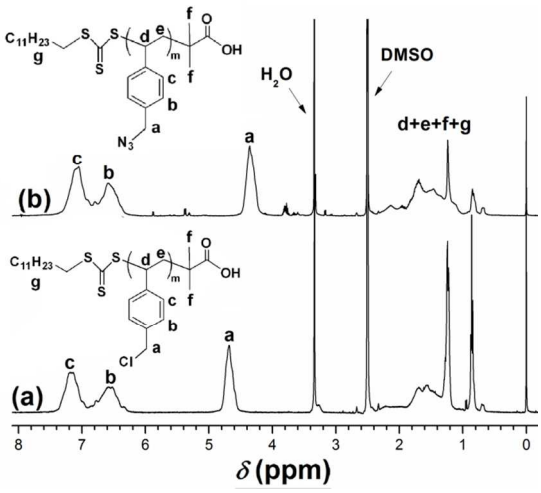


**Fig. 1** $^1$H NMR of (a) PCMS and (b) PAMS in DMSO-$d_6$.

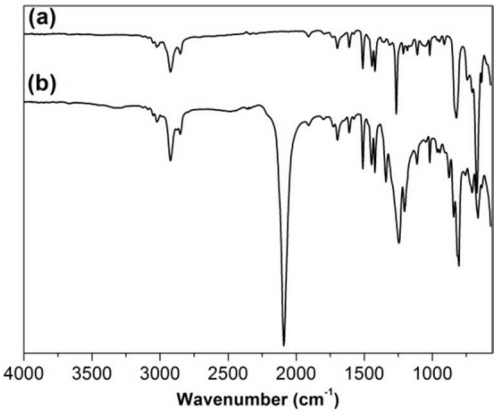


**Fig. 2** ATR FT-IR spectra of (a) PCMS and (b) PAMS.

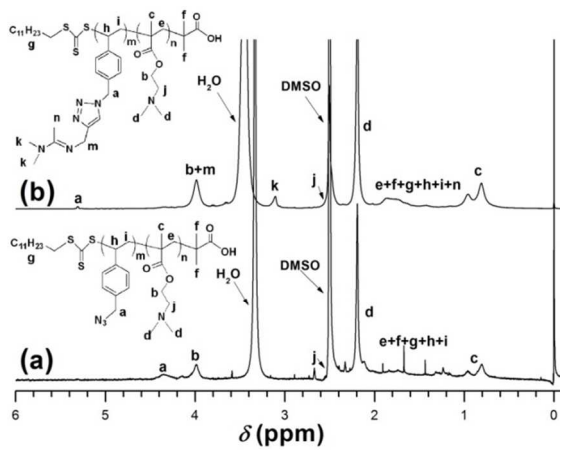


**Fig. 3** $^1$H NMR of (a) PAMS-*b*-PDMAEMA and (b) PADS-*b*-PDMAEMA in DMSO-$d_6$.

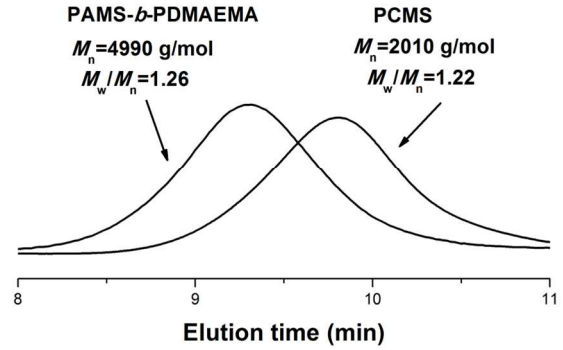


**Fig. 4** GPC traces of PCMS and PAMS-*b*-PDMAEMA.

### Self-assembly behaviour of the PADS-*b*-PDMAEMA copolymer

PADS-*b*-PDMAEMA could self-assemble to vesicles due to the amphiphilic nature of the copolymer, in which the PDMAEMA portion is hydrophilic and the PADS portion is hydrophobic at room temperature and in neutral aqueous solution. The critical aggregation concentration (CAC) was measured by the fluorescent probe method according to the literature.[31] The value of CAC for the PADS-*b*-PDMAEMA copolymer is approximately 0.047 mg mL$^{-1}$ as shown in Fig. 5.

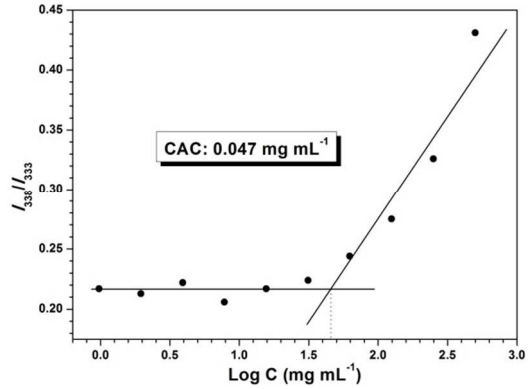


**Fig. 5** Critical aggregation concentration (CAC) of PADS-*b*-PDMAEMA copolymer.

The aggregates of PADS-*b*-PDMAEMA in aqueous solutions were investigated by transmission electron microscopy (TEM) and dynamic light scattering (DLS). It can be seen in Fig. 6(a) that the self-assemblies show spherical morphology. The clear contrast between the dark periphery and the hollow centre indicates that these spheres are vesicular. At 25°C and in neutral aqueous solution, the average size of the vesicles is about 500 nm, which is consistent with the hydrodynamic radius ($R_h$) of 244.8 nm determined by DLS as shown in Fig. 7 (a). In view of the good agreement, this image is used to evaluate the wall thickness, which statistically yields a thickness of (114 ± 8) nm.

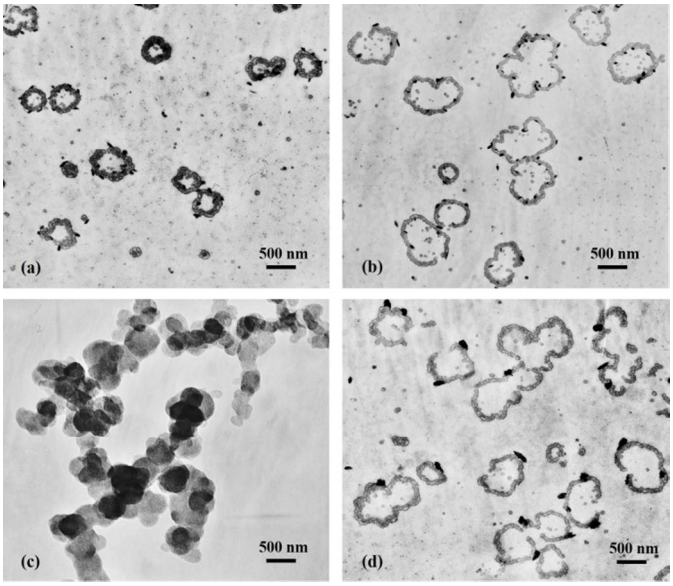


**Fig. 6** TEM images of (a) PADS-*b*-PDMAEMA vesicles at 25°C without bubbling $CO_2$, (b) PADS-*b*-PDMAEMA vesicles at 25°C after bubbling $CO_2$ for 20 min, (c) PADS-*b*-PDMAEMA micelles/aggregates after heating to 45°C and without bubbling $CO_2$, (d) PADS-*b*-PDMAEMA vesicles after heating to 45°C and bubbling $CO_2$ for 20 min (concentration: 1mg/mL).

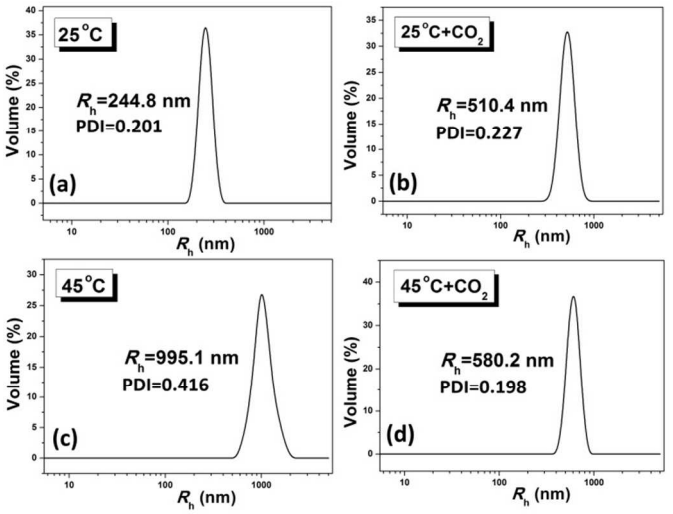


**Fig. 7** Hydrodynamic radius ($R_h$) of PADS-*b*-PDMAEMA aqueous solutions at different conditions: (a) 25°C, (b) 25°C and $CO_2$, (c) 45°C and (d) 45°C and $CO_2$ (concentration: 1mg/mL).

**$CO_2$- and thermo-responsive behaviours of the PADS-*b*-PDMAEMA vesicles**

It is worth noting that these vesicles can expand when $CO_2$ is passed through the PADS-*b*-PDMAEMA solution. As shown in Fig. 6(b), much larger vesicles with a diameter of ~1000 nm were observed after $CO_2$ treatment for 1200 s. For these aggregates, the value of $R_h$ is 510.4 nm, as determined by DLS (Fig. 7(b)), corresponding to the TEM results. Compared with its counterpart without gas stimulus (Fig. 6(a)), the volume of these new vesicles after gas stimulus increased strikingly and the wall thickness decreased to (83 ± 5) nm.

At low temperature and neutral conditions, PDMAEMA is water-soluble due to its hydrophilic tertiary amine and carbonyl groups. Upon bubbling $CO_2$ at room temperature, the reaction of PDMAEMA with $CO_2$ in water results in the protonation of the amine groups by carbonic acid, which leads to the formation of charged and more water-soluble ammonium bicarbonates. At the same time, the amidine groups in PADS block also transform into charged amidinium species upon reaction with $CO_2$, leading to the obvious increase of hydrophilicity of PADS segments. As a result, the vesicles expanded distinctly. It is noteworthy that the vesicles not only swelled but also partly ruptured and fused into larger vesicles when the PDMAEMA and PADS segments were transformed into polyelectrolyte upon $CO_2$ treatment according to TEM image of Fig. 6(b), which should be attributed to the protonation of PDMAEMA and PADS in $CO_2$ environment.

The protonation process of PDMAEMA and PADS is related with the bubbling time of $CO_2$ to aqueous solution. The PDMAEMA chains in hydrophilic layer of vesicles become more spread and the hydrophobic wall of vesicles becomes looser due to the hydrophobic-hydrophilic transition of PADS chains. As shown in Fig. 8(a), the expansion of vesicles upon $CO_2$ bubbling undergoes two stages. The first stage is ranged from 0 to 300 s. The $R_h$ value of the vesicles dramatically increased from 224 nm to 455 nm. The second stage is from 300 to 1200 s. At this stage, the $R_h$ value of the vesicles only moderately increased from 455 nm to 512 nm. This time dependence increase of $R_h$ is mainly due to the equilibrium property of the reaction for PADS block and PDMAEMA block with $CO_2$ in aqueous solution. The $R_h$ of the vesicles increases dramatically, resulting from the protonation of PADS and PDMAEMA, when bubbling $CO_2$ to the aqueous solution for the first 300 s. However, since the reaction of PADS and PDMAEMA with $CO_2$ in aqueous solution is an equilibrium reaction, the protonation of PADS and PDMAEMA would reach the equilibrium state when bubbling $CO_2$ for a certain time. Thus, the $R_h$ of the vesicles increases moderately from 300 to 1200 s.

For these vesicles, the gas-response is reversible. After bubbling Ar, the expanded vesicles would shrink into vesicles with original size. The change tendency during bubbling Ar process is contrary to that of during bubbling $CO_2$ process. As shown in Fig. 8(a), the $R_h$ value decreased from 520 nm to 230 nm after bubbling Ar to the vesicle solution for 1200 s. It can be explained that the protonation of amindine groups in PADS and dimethylamino groups in PDMAEMA is weakened after passing Ar to the vesicle solution, and the loose chain conformation in vesicles converts to tighten state.

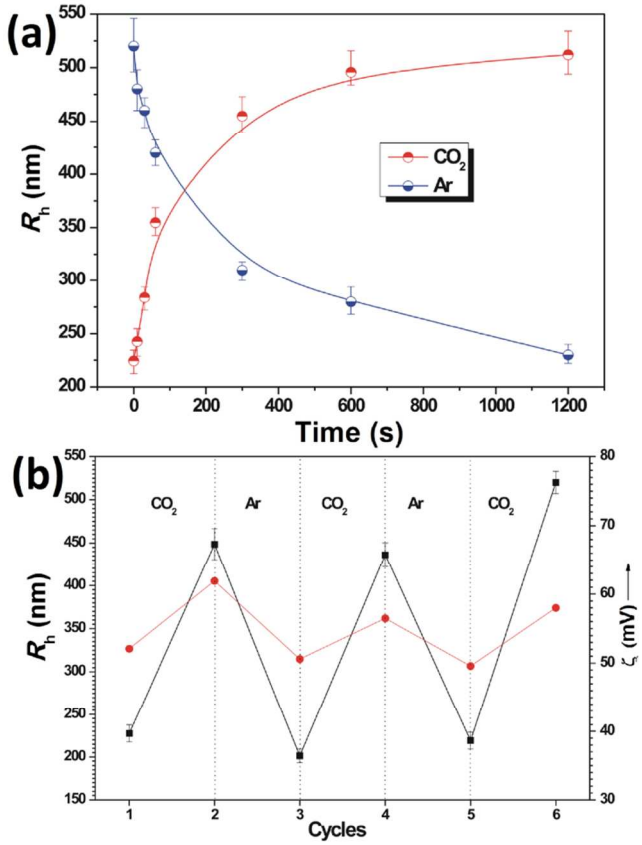


**Fig. 8** (a) Time dependence of the hydrodynamic radius ($R_h$) for PADS-*b*-PDMAEMA vesicles under $CO_2$ or Ar exposure and (b) the reversible $R_h$ (black) and Zeta potential (red) change of PADS-*b*-PDMAEMA vesicles with circular bubbling $CO_2$ or Ar (concentration: 1mg/mL).

The reversible $R_h$ and Zeta potential change of PADS-*b*-PDMAEMA vesicles with circular bubbling $CO_2$ or Ar are shown in Fig. 8(b). The initial $R_h$ of the vesicles was 227 nm, and the $R_h$ rapidly increased to 448 nm after bubbling $CO_2$ for 5 min. The protonation of PADS and further protonation of PDMAEMA led to the loose and partial breakage of vesicles. After bubbling Ar to the vesicle solution for 5 min, PADS and PDMAEMA segments were deprotonated. The $R_h$ rapidly decreased to 201 nm. Subsequently, the $R_h$ values underwent circulation changes according to the alternation of bubbling $CO_2$/Ar. The results indicated that the copolymer vesicles could realize the reversible shrinkage-expansion transition. Moreover, a zeta potentiometer was employed to investigate the change of surface charge of the vesicles. Before $CO_2$ was added, the solution had a signal ($\zeta_{CO2}$ = +52.1 mV), indicating that the initial vesicles carried relatively high surface charges due to the partial protonation of PDMAEMA at pH 7.0. The value of $\zeta_{CO2}$ progressively climbed to +61.9 mV upon $CO_2$ treatment for 5 min. At this time, the vesicle solution presented weak acidity

(pH 6.36). After bubbling Ar for 5 min, the value of $\zeta_{CO2}$ decreased to 50.6 mV owing to the partial deprotonation of PDMAEMA and PADS. It can be seen that the surface charges reversibly changed with the alternative bubbling $CO_2$/Ar and the change tendency was in accordance with the change of $R_h$ of copolymer vesicles, further revealing that the protonation/deprotonation transformation of PADS and PDMAEMA segments led to the morphology change of the vesicles.

When the solution was heated to 45°C, the vesicles were transformed into aggregates composed of micelles, as shown in Fig. 6(c). Without charging $CO_2$ and the temperature above LCST of PDMAEMA segments, PADS and PDMAEMA both became hydrophobic chains. As a result, the vesicles transformed into micelles and the unstable micelles tended to aggregate into aggregates with large size. This process is depicted in Scheme 2. However, the micelle aggregates transformed into expanded vesicles when $CO_2$ was bubbled for 5 min at 45°C, just like the morphology shown in Fig. 6(b). Compared to the $R_h$ of the vesicles at 25°C (Fig. 7(a)) and after bubbling $CO_2$ for 5 min (Fig. 7(b)), the size of $R_h$ of the micelle aggregates at 45°C (Fig. 7(c)) and the vesicles after bubbling $CO_2$ (5 min, 45°C) (Fig. 7(d)) increased. The reason is mainly that the LCST of PDMAEMA segments has been improved above 45°C after bubbling $CO_2$ for 5 min and the PDMAEMA block is hydrophilic at such condition. Meanwhile, the hydrophilicity of PADS block increased as the amidine groups transform into charged amidinium species after reaction with $CO_2$. As a result, the aggregates transformed into expanded vesicles.

Fig. 9(a) shows the transmittance curves of PADS-*b*-PDMAEMA aqueous solutions at different conditions. It can be seen that the transmittance curve presents sharp transition during heating process for the initial solution and the LCST value of the copolymer was 42.8°C. After bubbling $CO_2$ into the solution for 20 min, the transmittance increased to ~78% and no obvious transition occurred during the process of heating. After passing Ar through the solution for 20 min, the sharp transition during heating process appeared again and the LCST value was 43.6°C.

The plot of the hydrodynamic radius ($R_h$) of PADS-*b*-PDMAEMA self-assemblies in aqueous solutions as a function of temperature is shown in Fig. 9(b). In the lower temperature ranges, the $R_h$ values were relatively small and changed slightly. When the temperature continued to increase, the $R_h$ values decreased to some extent. But in the higher temperature ranges, the $R_h$ values increased rapidly. The above changes are due to the thermal response of PDMAEMA block. At lower temperatures, the PDMAEMA chains in the PADS-*b*-PDMAEMA copolymer existed in random coil conformation owing to the hydrogen-bonding interaction between the N,N-dimethylaminoethyl groups of PDMAEMA chains and water molecules. When the temperature continued to increase, the PDMAEMA chains would shrink into a globular structure as the hydrogen bonds were obviously weakened or broken. Therefore, the PDMAEMA chains collapsed and the $R_h$ value decreased. When the temperatures increased to higher ranges, the PDMAEMA chains became more hydrophobic and the intermolecular hydrophobic attractions are thermodynamically favoured. Thus aggregation occurred, which results in the rapid increase in $R_h$. After bubbling $CO_2$ into the solution for 20 min, the $R_h$ values increased obviously and changed slightly in the heating process, resulting from the protonation of PDMAEMA and PADS blocks. The protonation of the amine groups of PDMAEMA would make the block charged and more water-soluble, and the hydrophilicity of PADS block would increase after protonation. As a result, the vesicles expanded and the $R_h$ values increased distinctly. Meanwhile, the protonated amine groups made the PDMAEMA chains remain hydrophilic at high temperature. So the aggregation would not occur in high temperature ranges and the $R_h$ values presented unobvious change in the heating process. However, after Ar was passed through the solution, $CO_2$ would be expelled by Ar and the protonated PADS-*b*-PDMAEMA returned to the initial state. Therefore, PDMAEMA chains collapsed and the aggregation happened with the increase of temperature.

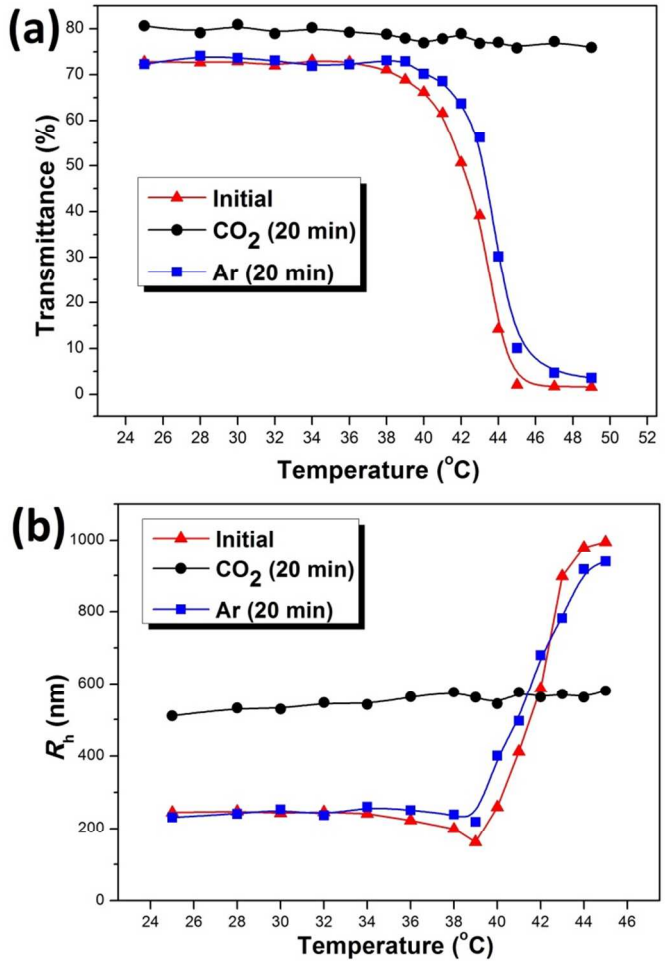


**Fig. 9** (a) Transmittance curves and (b) temperature dependence of hydrodynamic radius ($R_h$) of PADS-*b*-PDMAEMA aqueous solutions at different conditions (concentration: 1 mg/mL).

**Controlled drug release of the PADS-*b*-PDMAEMA vesicles**

Since the vesicles presented obviously $CO_2$- and temperature-responsive properties, they could be used in controlled drug-delivery system. DOX, a typical anticancer drug, was used as model drug to investigate the controlled release behaviour of the vesicles. The DOX is located in the hydrophobic PADS membrane of the vesicles due to the hydrophobic interaction between DOX and the PADS block.[32, 33] The standard curve of DOX is shown in Fig. S1 and the drug loading content (DLC) and drug loading efficiency (DLE) were 6.4% and 22.6%, respectively. Fig. 10(a) shows the drug-release curves of PADS-*b*-PDMAEMA vesicles at different conditions. It can be found that the DOX release from vesicles at 25°C was slow, and only 15.5% of DOX was released from the vesicles within 40 h. The low release of DOX is mainly because the interaction between DOX and PADS-*b*-PDMAEMA copolymer. Besides the hydrophobic interaction between DOX and PADS chains, DOX, due to its special chemical constitution, has interaction with PDMAEMA chains in aqueous solutions at the same time. Thus the release of DOX is hindered and the release level is quite low. The low release of DOX also indicates the stability of the copolymer vesicles at room temperature. After bubbling $CO_2$ into the vesicle solution for 5 min, the release amount of DOX increased to 23.0% after 40 h. This increase should attribute to the expansion and deformation of the vesicles. The loose chains were beneficial to the diffusion of DOX from the vesicles. At 45°C, the cumulative release amount increased rapidly to 34.7% within 5 h and reached 55.9% after 30 h. In this condition, the vesicles transformed to micelle aggregates as PDMAEMA block became hydrophobic at the temperature higher than its LCST. The transformation and reorganization of the copolymer self-assemblies and the increase of thermo-motion together resulted in the rapid release of DOX molecules from the copolymer aggregates. Furthermore, the release amount of DOX at 45°C and after bubbling $CO_2$ for 5 min is lower than that at 45°C without bubbling $CO_2$. This result may attribute to the morphology difference of the physical aggregates between the two conditions. The self-assemblies at "45°C" condition are micelle aggregates (Fig. 6(c)), while the aggregate at "45°C+$CO_2$" condition is vesicles (Fig. 6(d)). Moreover, it should be noticed that the PDMAEMA chains shrank into a globular structure and collapsed at "45°C" condition because the hydrogen bonds between the dimethylamino groups of PDMAEMA and water molecules are weakened at this temperature. After bubbling $CO_2$, the shrunken PDMAEMA chains expanded because of the protonation of dimethylamino groups. So the coronas of the micelle aggregates at "45°C" condition are thinner than that of the vesicles at "45°C+$CO_2$" condition, thus resulting in the faster release of DOX. Meanwhile, the release rate of DOX at 45°C and after bubbling $CO_2$ for 5 min (45°C+$CO_2$) is higher than that at 25°C and after bubbling $CO_2$ for 5 min (25°C+$CO_2$). It is mainly because that in this condition (45°C+$CO_2$), the vesicles were expanded and PDMAEMA segments were hydrophilic. The morphology of the vesicles was similar to that at 25 °C and after bubbling $CO_2$ for 5 min (25°C+$CO_2$). But the increase of thermo-motion at higher temperature enhanced the diffusion of DOX from the expanded vesicles.

Fig. 10 (b) shows the controlled release of DOX from PADS-b-PDMAEMA vesicles without stimuli and with alternating $CO_2$/Ar stimuli. Compared to the release curve of DOX at 25°C, the release curve with alternative $CO_2$/Ar bubbling presented a periodic fast-slow alternation feature, which should attributed to the extension-retraction motion of the vesicles under the alternative stimulation of $CO_2$/Ar.

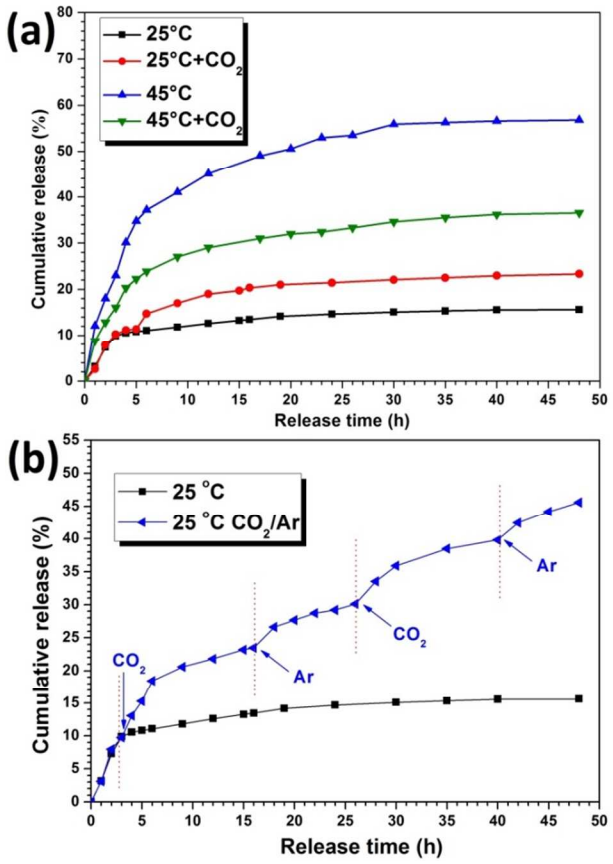


**Fig. 10** (a) Controlled release of DOX from PADS-*b*-PDMAEMA vesicles or micelles/aggregates at different conditions and (b) controlled release of DOX from PADS-*b*-PDMAEMA vesicles without stimuli and with alternating $CO_2$/Ar stimuli.

## Conclusions

A novel amidine- and dimethylamino-containing block copolymer (PADS-*b*-PDMAEMA) was synthesized by the combination of RAFT and click chemistry. The copolymer can spontaneously form vesicles in aqueous media on the basis of its amphiphilicity. The amidine and dimethylamino groups in the copolymer endow the vesicles with unique dual $CO_2$ responses. The size and morphologies of these vesicles can be adjusted by controlling the protonation/deprotonation of amidine and dimethylamino species. Alternating treatment with $CO_2$ and Ar could realize a smart expansion and contraction cycle of these vesicles. Meantime, the PADS-*b*-PDMAEMA copolymer showed typically thermo-responsive properties and

the LCST value is 42.8°C without bubbling $CO_2$. After bubbling $CO_2$, there is no obvious change of the transmittance in the process of heating due to the protonation of dimethylamino groups in PDMAEMA. Removing $CO_2$ by Ar would result in the appearance of the similar LCST value (43.6°C). Moreover, the reversible vesicles-micelles transition could also be achieved through stimuli of temperature and gas. As a carrier for drugs, the vesicles presented good controlled release behaviour. The release rate and level could be controlled through bubbling $CO_2$ and changing temperature.

## Acknowledgements

The authors are grateful for the financial support of the National Basic Research Program of China (973 Program: 2011CB013805), the National Key Technology R&D Program (no.2012BAI15B061), and the National High Technology Research and Development Program (no. 2013AA032202).

## Notes and references

[a]Institute of Nano and Bio-polymeric Materials, School of Materials Science and Engineering, Tongji University, 4800 Cao'an Road, Shanghai 201804, People's Republic of China. Fax: +86 21 69584723; Tel: +86 21 69580234; E-mail: yuanwz@tongji.edu.cn

[b]Key Laboratory of Advanced Civil Materials, Ministry of Education, 4800 Cao'an Road, Shanghai 201804, People's Republic of China. Fax: +86 21 69584723; Tel: +86 21 69580234; E-mail: yuanwz@tongji.edu.cn.

Electronic Supplementary Information (ESI) available. See DOI: 10.1039/b000000x/

1 Z. S. Ge and S. Y. Liu, *Chem. Soc. Rev.*, 2013, **42**, 7289-7325.

2 C. Alvarez-Lorenzo and A. Concheiro, *Chem. Commun.*, 2014, **50**, 7743-7765.

3 M. Huo, J. Y. Yuan, L. Tao and Y. Wei, *Polym. Chem.*, 2014, **5**, 1519-1528.

4 W. Z. Yuan, H. Zou, W. Guo, T. X. Shen and J. Ren, *Polym. Chem.*, 2013, **4**, 2658-2661.

5 W. Z. Yuan and W. Guo, *Polym. Chem.*, 2014, **5**, 4259-4267.

6 N. Ma, Y. Li, H. P. Xu, Z. Q. Wang and X. Zhang, *J. Am. Chem. Soc.*, 2010, **132**, 442-443.

7 A. C. Feng, C. B. Zhan, Q. Yan, B. W. Liu and J. Y. Yuan, *Chem. Commun.*, 2014, **50**, 8958-8961.

8 X. L. Hu, H. Li, S. Z. Luo, T. Liu, Y. Y. Jiang and S. Y. Liu, *Polym. Chem.*, 2013, **4**, 695-706.

9 G. Liu, W. Liu and C. M. Dong, *Polym. Chem.*, 2013, **4**, 3431-3443.

10 Y. Z. You, C. Y. Hong and C. Y. Pan, *Macromolecules*, 2009, **42**, 573-575.

11 D. H. Han, O. Boissiere, S. Kumar, X. Tong, L. Tremblay and Y. Zhao, *Macromolecules*, 2012, **45**, 7440-7445.

12 B. W. Liu, H. Zhou, S. T. Zhou, H. J. Zhang, A. C. Feng, C. M. Jian, J. Hu, W. P. Gao and J. Y. Yuan, *Macromolecules*, 2014, **47**, 2938-2946.

13 Q. Yan, R. Zhou, C. K. Fu, H. J. Zhang, Y. W. Yin and J. Y. Yuan, *Angew. Chem. Int. Ed.*, 2011, **50**, 4923-4927.

14 Y. Ding, S. L. Chen, H. P. Xu, Z. Q. Wang and X. Zhang, *Langmuir*, 2010, **26**, 16667-16671.

15 Z. R. Guo, Y. J. Feng, Y. Wang, J. Y. Wang, Y. F. Wu and Y. M. Zhang, *Chem. Commun.*, 2011, **47**, 9348-9350.

16 J. Pinaud, J. Vignolle, Y. Gnanou and D. Taton, *Macromolecules*, 2011, **44**, 1900-1908.

17 Q. Yan, J. B. Wang, Y. W. Yin and J. Y. Yuan, *Angew. Chem. Int. Ed.*, 2013, **52**, 5070-5073.

18 Z. R. Guo, Y. J. Feng, S. He, M. Z. Qu, H. L. Chen, H. B. Liu, Y. F. Wu and Y. Wang, *Adv. Mater.* 2012, **3**, 25, 584-590.

19 Y. Liu, P. G. Jessop, M. Cunningham, C. A. Eckert and C. L. Liotta, *Science*, 2006, **313**, 958-960.

20 T. Yu, R. Cristiano and R. G. Weiss, *Chem. Soc. Rev.*, 2010, **39**, 1435-1447.

21 Q. Yan and Y. Zhao, *Angew. Chem. Int. Ed.*, 2013, **52**, 9948-9951.

22 D. H. Han, X. Tong, O. Boissière and Y. Zhao, *ACS Macro Lett.*, 2012, **1**, 57-61.

23 J. Pinaud, E. Kowal, M. Cunningham and P. Jessop, *ACS Macro Lett.*, 2012, **1**, 1103-1107.

24 Q. Zhang, G. Q. Yu, W. J. Wang, B. G. Li and S. P. Zhu, *Macromol. Rapid Commun.*, 2012, **33**, 916-921.

25 B. Yan, D. H. Han, O. Boissière, P. Ayotte and Y. Zhao, *Soft Matter*, 2013, **9**, 2011-2016.

26 J. T. Lai, D. Filla and R. Shea, *Macromolecules*, 2002, **35**, 6754-6756.

27 W. Z. Yuan, H. Zou, W. Guo, T. B. Ren and J. Ren, *Polym. Bull.*, 2013, **70**, 2257-2267.

28 W. Z. Yuan, X. F. Li, S. Y. Gu, A M. Cao and J. Ren, *Polymer*, 2011, **52**, 658-666.

29 S. Amajjahe, S. Choi, M. Munteanu and H. Ritter, *Angew. Chem. Int. Ed.*, 2008, **47**, 3435-3437.

30 X. J. Wan, T. Liu and S. Y. Liu, *Biomacromolecules*, 2011, **12**, 1146-1154.

31 L. D. Feng, H. Yu, Y. C. Liu, X. Y. Hu, J. J. Li, A M. Xie, J. F. Zhang and W. Dong, *Polym. Chem.*, 2014, **5**, 7121-7130.

32 A. Car, P. Baumann, J. T. Duskey, M. Chami, N. Bruns and W. Meier, *Biomacromolecules*, 2014, **15**, 3235-3245.

33 Y. Zhang, J. L. He, D. L. Cao, M. Z. Zhang and P. H. Ni, *Polym. Chem.,* 2014, **5**, 5124-5138.

# Graphical Abstract

The vesicles present dual $CO_2$-responses and would undergo reversible vesicles-micelles transition upon thermo and $CO_2$ stimulations.